

# Highly Stable Silver Nanoplates for Surface Plasmon Resonance Biosensing\*\*

Chuanbo Gao, Zhenda Lu, Ying Liu, Qiao Zhang, Miaofang Chi, Quan Cheng, and Yadong Yin\*

Surface plasmon resonance (SPR) spectroscopy is a versatile method for probing the binding of biomolecules through the changes in refractive index occurring on thin metal films.<sup>[1]</sup> One of the main drawbacks that impede further development of SPR applications is the lack of sufficient sensitivity to reliably detect small changes in refractive index caused by compounds with low molecular weight or in low concentration at the sensing surface.<sup>[2]</sup> Several approaches have been reported to address such limitations. Specifically, Au nanoparticles, the localized SPR of which can be coupled with that of a thin metal surface, were extensively explored to enhance SPR response in biosensors.<sup>[3]</sup>

Compared with Au, nanoparticles of Ag produce a much stronger and sharper plasmon resonance,<sup>[4]</sup> which in principle promises a wider range of potential applications, including not only chemical and biological sensing,<sup>[5]</sup> but also imaging<sup>[6]</sup> and catalysis.<sup>[7]</sup> It has been long recognized that the use of Ag may lead to more sensitive SPR-sensing devices than Au.<sup>[8]</sup> However, poor chemical and structural stability has been the main issue that prevents broad use of Ag in place of Au in SPR sensing, because the structures and plasmonic properties of Ag nanoparticles are subject to changes when exposed to water,<sup>[9]</sup> acids,<sup>[10]</sup> halides,<sup>[11]</sup> oxidative agents, UV irradiation,<sup>[12]</sup> and heat.<sup>[13]</sup> As a result, direct application of Ag nanoparticles as amplified labels (enhancers) in SPR sensing has been rarely reported. As an alternative method, the so-called silver enhancement technique has sometimes been used to enhance the SPR signal by selective deposition of Ag on Au nanoparticles labeled with the target specimen,<sup>[14]</sup> which, however, suffers from complicated procedures and high background signal from nonspecific silver deposition.

It is therefore essential to develop strategies to stabilize Ag nanostructures while retaining their excellent plasmonic properties for use as effective enhancers in SPR sensing. A conventional approach is to modify the surface of the Ag nanostructures with an extra protecting layer of inorganic or organic material, such as silica,<sup>[15]</sup> Au,<sup>[16]</sup> and self-assembled monolayers (SAMs) of organic thiols,<sup>[9,17]</sup> to prevent direct contact of Ag with external etchants. Although the stability of the protected Ag nanostructures has been improved to some extent, these existing methods are still problematic. For example, burying the active Ag surface in an inert silica layer provides limited protection against etching, but limits access of the target molecules to the Ag surface and consequently reduces the sensing efficiency. Au deposition, which is typically achieved by galvanic replacement, is initiated at specific sites of a Ag nanoparticle, so that the system is stable only under very mild conditions because of partial Au coverage.<sup>[16a]</sup> A thick Au shell that is produced through galvanic replacement and subsequent refilling may further enhance the stability, but can also limit use for SPR sensing, as the plasmonic properties become dominated by Au.<sup>[16b]</sup> Thiol-based organic molecules oxidize the surface of Ag, thus causing a large decrease in the plasmonic activity and problems for further surface derivatization.

An ideal protecting layer should provide sufficient protection against disturbance from the environment over a reasonably long period, but should not significantly alter the plasmonic property and surface characteristics of the original nanostructures. Herein, we report a novel method to produce highly stable Ag nanoplates and demonstrate their superior performance in SPR sensing of proteins. The Ag nanoplates are stabilized by uniformly depositing a very thin layer of Au to form an Ag@Au core/shell nanostructure without significant involvement of galvanic replacement, and thus the plasmonic property of the Ag nanostructures is retained. The exposed Au surface provides opportunities for further chemical modifications for SPR biosensing.

The key to uniformly depositing a thin layer of Au on the Ag nanoplates is to minimize galvanic replacement. In addition to its destructive etching effect on the original Ag nanostructures, which dramatically changes the optical property,<sup>[18]</sup> galvanic replacement also leads to nonuniform deposition of Au because the reaction is initiated only locally at certain high-energy sites.<sup>[19]</sup> To minimize galvanic replacement, we first decreased the reduction potential of the Au salt by complexation with I<sup>-</sup> to +0.56 V (versus standard hydrogen electrode, SHE),<sup>[20]</sup> which is much lower than those for Au ions ( $E^\circ(\text{Au}^{3+}) = +1.52$ ,  $E^\circ(\text{AuCl}_4^-) = +0.93$  V versus SHE). Second, we introduced polyvinylpyrrolidone (PVP) as an

[\*] Dr. C. Gao, [†] Z. Lu, [‡] Y. Liu, [§] Q. Zhang, Prof. Q. Cheng, Prof. Y. Yin  
Department of Chemistry, University of California  
Riverside, CA 92521 (USA)  
E-mail: yadong.yin@ucr.edu  
Homepage: <http://faculty.ucr.edu/~yadong/>

Dr. M. Chi  
Materials Science Division, Oak Ridge National Laboratory  
Oak Ridge, TN 37830 (USA)

[†] These authors contributed equally to this work.

[\*\*] This work was supported by the National Science Foundation under Grant Nos. DMR-0956081 (Y.Y.) and CHE-1059050 (Q.C.). Y.Y. also thanks the Research Corporation for Science Advancement for the Cottrell Scholar Award and DuPont for the Young Professor grant. Part of the TEM work was performed at ORNL's Shared Research Equipment (SHaRE) User Facility, which is sponsored by the Office of Basic Energy Sciences, U.S. DOE.

Supporting information for this article is available on the WWW under <http://dx.doi.org/10.1002/ange.201108971>.

additional ligand to stabilize the silver against replacement by gold ions, by taking advantage of the strong coordination between the O and N atoms of the pyrrolidone ring and the metallic silver surface.<sup>[16b,17,21]</sup> Because PVP molecules are known to be preferentially adsorbed on the (100) facets,<sup>[22]</sup> we also introduced a small amount of diethylamine to help eliminate the energy difference for etching/deposition between different facets of silver. Since diethylamine is known to be unselectively adsorbed on the surface of Ag nanoparticles without causing etching, we can ensure homogeneous Au deposition on the surface of the Ag nanoparticles.<sup>[15,20]</sup>

In a typical synthesis of Au-stabilized Ag nanoparticles, an aqueous solution containing HAuCl<sub>4</sub>, KI, and PVP was first prepared as a growth solution, which was then slowly added to a mixture containing PVP, diethylamine, ascorbic acid, and Ag nanoparticles.<sup>[21,22b]</sup> In addition to the function of PVP as a capping ligand for stabilizing silver nanoparticles and preventing aggregation of the final products, our earlier work suggested that PVP might also help to stabilize the Au “monomers” resulting from the initial reduction, and thus minimize the possibility of self-nucleation.<sup>[20]</sup>

Figure 1a shows a typical transmission electron microscopy (TEM) image of the Ag@Au core/shell nanoparticles. The original triangular/hexagonal shapes are well retained, as expected by the uniform deposition of Au atoms on the plate surface. Some plates contain small voids on their surfaces, thus suggesting that galvanic replacement, although greatly minimized, can still occur at the early stage. However, unlike the reactions driven predominantly by galvanic replacement, in which only a small amount of Au can be deposited at the edges before incurring structural damage to the plate body, thus resulting in very limited protection,<sup>[16a]</sup> in this work the thickness of Au can be continuously and uniformly increased by adding more growth solution, without causing problematic changes to the plate structure.

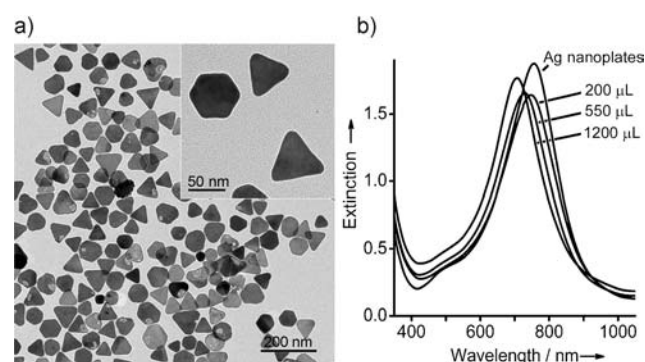


**Figure 1.** a) TEM image of the Ag@Au core/shell nanoparticles. b) UV/Vis/NIR spectra of the original Ag nanoparticles and Ag@Au core/shell nanostructures prepared by adding various amounts of Au growth solution.

Most importantly, the plasmonic property can be maintained during Au coating, as monitored by UV/Vis/NIR spectroscopy (Figure 1b). The intensity of the in-plane dipole plasmon of Ag nanoparticles at about 755 nm first decreased slightly because of the coverage of the Ag surface by Au, and

afterwards increased because of continuous deposition of the Au layer and thus increased quantity of plasmonic materials. The final intensity of the plasmon band is close to that of the original Ag nanoparticles, thus suggesting that the plasmonic property of the Ag nanoparticles has been mostly retained. The position of the plasmon band shifted to the blue during Au deposition, which can be explained by a decrease in the aspect ratio of the plate structure. The blueshift of the plasmonic peak suggests that the reaction is dominated by deposition, which is completely different from prior works in which the plasmonic peak shifts to the red because the plates were made thinner during galvanic replacement.<sup>[16a]</sup> Furthermore, the plasmon band of the Ag nanoparticles quickly decreases in intensity during typical galvanic replacement because of the loss of more plasmonically active silver species,<sup>[18a]</sup> which is distinct from our reaction.

The Ag@Au core/shell nanoparticles were further characterized by high-resolution scanning transmission electron microscopy (STEM) to investigate the distribution of Au atoms (Figure 2a,b). The dark-field STEM image (Figure 2b), which is essentially a Z (atomic number)-contrast image, shows a relatively bright edge surrounding the nanoplate. An intensity profile across the edge of the nanoplate clearly shows such increased contrast, and indicates deposition of a thin layer of Au on the Ag nanoplate surface. The average thickness of the Au shells was measured to be about 5 Å, which corresponds to approximately four layers of Au atoms. Besides the economic benefits, a thin coating ensures that the plasmonic property of the Ag core does not decay

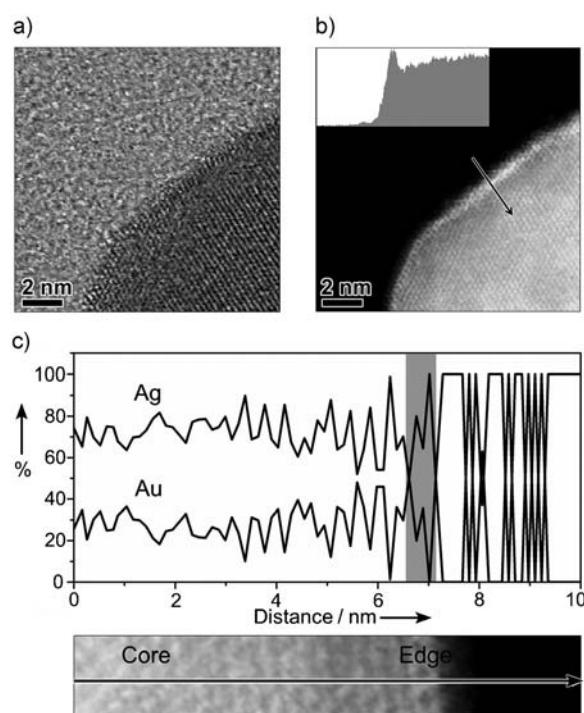


**Figure 2.** a, b) Bright-field and dark-field STEM images of a Ag@Au nanoparticle. Inset: intensity profile of a line scan indicated by the arrow. c) Atomic percentage profile of a Ag@Au nanoplate calculated from the relative counts in the EDS line scan indicated by the arrow in the STEM image below.

significantly because of Au coverage. Furthermore, both the bright-field and dark-field STEM images suggest a good lattice match between the Au layer and the Ag core, which favors effective isolation of the Ag nanostructures from their external environment and thus high stability.

High-resolution energy-dispersive X-ray spectroscopy (EDS) further confirmed such Ag(core)/Au(shell) structure. A typical EDS line scan across the surface of a single nanoplate is shown in Figure 2c. In the bulk area of the nanoplate, the presence of both Ag and Au was detected, thus suggesting that the Au has been deposited on the faces of the original nanoplates. The atomic percentage of Au is about 26% on average, which is close to the theoretical value of 21%, assuming 100% yield of both Ag and Au during the synthesis. About 0.5 nm from the edge of the nanoplates, the atomic percentage of Ag drops to zero and that of Au rises to 100%, which is consistent with the fact that the edge Au atoms are deposited through reduction of Au cations instead of partial replacement of Ag.

As the atomic layers of Au are uniformly deposited on the Ag surface with minimal galvanic replacement, these nanoplates are highly stable against chemical etching. Figure 3a–c

shows the change of the plasmonic bands of Ag@Au nanoplates, as monitored by UV/Vis/NIR spectroscopy over time, in a phosphate buffer solution, a NaCl solution, and a phosphate-buffered saline (PBS) solution, respectively. In all cases, the position and the intensity of the in-plane dipole plasmon resonance bands remained essentially unchanged for four days or longer. A slight decrease in peak intensity was observed after long storage in solutions that contain a high concentration of NaCl, which could be primarily attributed to aggregation of the nanoplates in a solution of high ionic strength. It is especially astonishing that the protected Ag nanoplates are highly stable even in  $\text{H}_2\text{O}_2$ , a strong oxidant that can easily destroy silver nanoplates protected by conventional methods (Figure 3d). Ag@Au nanoplates stored in  $\text{H}_2\text{O}_2$  for two hours appeared to be similar in morphology to the original Ag nanoplates (Figure 3d, inset), thus confirming their excellent stability against strong etching agents. Additionally, no obvious spectral change was observed when the Ag@Au nanoplates were irradiated by a large dose of UV light, that is, the Au layer can also effectively suppress migration of surface atoms.<sup>[12]</sup>

Control experiments were carried out for comparison. If

no protection was present, the original Ag nanoplates were quickly etched by PBS, NaCl, or  $\text{H}_2\text{O}_2$  (Figure 3e and Supporting Information), as evidenced by a significant shift in the peak position and a dramatic decrease in the intensity over a relatively short period. This is again the main reason that pristine Ag nanoplates have severe limitations in many practical applications in which salts, buffers, or oxidative agents are present. We found that the stability of Ag nanoplates protected by thiols, such as 16-mercaptohexadecanoic acid (MHA), was also very limited (Figure 3f).<sup>[17]</sup> The Ag–MHA nanoplates were only stable in a phosphate buffer solution without NaCl, while they gradually degraded in the presence of NaCl or  $\text{H}_2\text{O}_2$ . Furthermore, it is difficult to maintain a robust monolayer of MHA on the Ag surface when further derivatization is required.

The Ag nanoplates stabilized by Au coating are suitable for many bioanalytical applications. Herein, we demonstrate their excellent performance when used for enhancing SPR-based biosensing. We chose streptavidin as model protein. Briefly, our SPR biosensor detects biomolecules in a flow channel with a typical Kretschmann configuration: a thin Au film is deposited on a glass substrate, which is then attached to a prism. When a laser beam irradiates the Au substrate, the SPR angle, which characterizes the change in the refractive index on the thin Au film because of binding of target molecules, is determined and employed to quantify the

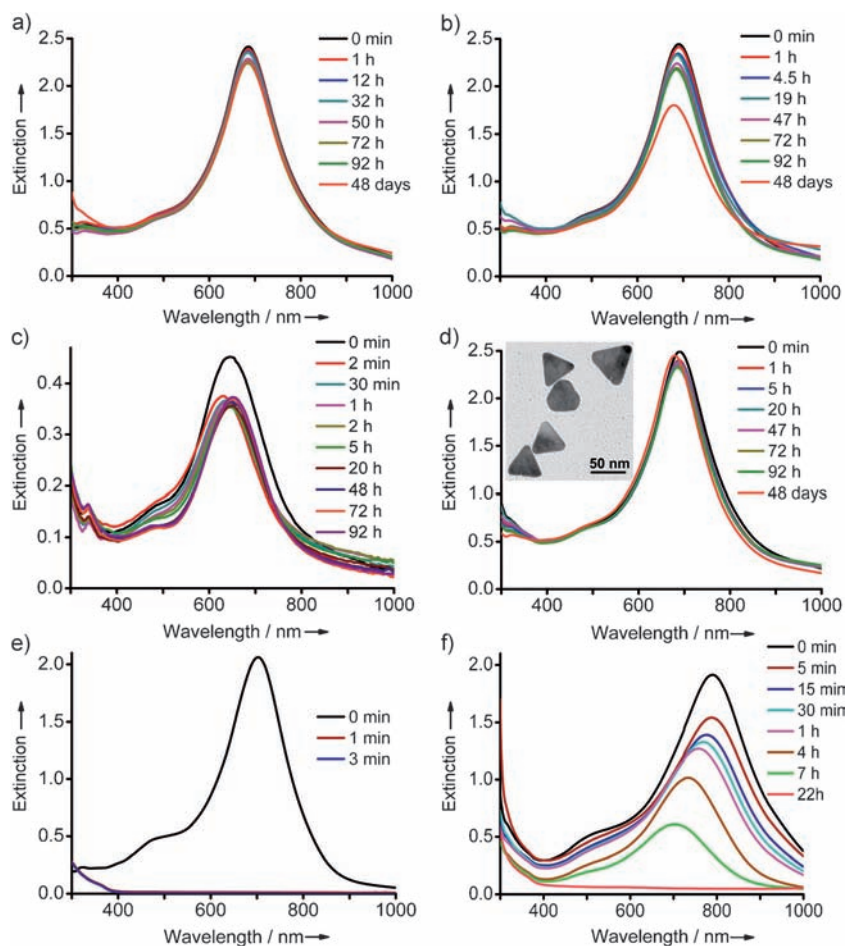


**Figure 3.** Stability of the Ag@Au nanoplates in a) phosphate buffer solution (10 mM, pH 7.4, PVP 0.5%), b) NaCl solution (20 mM, PVP 0.5%), c) PBS (10 mM, NaCl 150 mM, pH 7.4, PVP 0.5%), and d)  $\text{H}_2\text{O}_2$  solution (2.1%), monitored by UV/Vis/NIR spectrophotometry. A TEM image of the Ag@Au nanoplates after treatment in  $\text{H}_2\text{O}_2$  for 2 h is shown in the inset to (d). Stability of e) pristine Ag nanoplates and f) MHA-stabilized Ag nanoplates in  $\text{H}_2\text{O}_2$  (2.1%).



target molecules absorbed on the sensing surface. In a typical procedure, the Au film was modified with 11-mercaptopundecanoic acid (MUA), and the carboxy group of MUA was further coupled with biotin by amidation. Streptavidin was then injected to allow saturated absorption on the Au film through the specific biotin–streptavidin interaction. Finally, biotinylated Ag@Au nanoplates were introduced to enhance the SPR response. Throughout the process, the SPR angle was monitored for quantitative analysis.

In Figure 4a, the biotinylation of the Ag@Au nanoplates is illustrated. The Ag@Au nanoplates were first functionalized with MHA through Au–S bonds, and then covalently

plates completely lost their plasmonic property after biotinylation, and this suggests that the amidation reaction destroyed the coverage of the MHA monolayer and destabilized the Ag nanoplates.

Attachment of streptavidin on the Au surface only generated 0.05° of SPR signal (Figure 4c). After the surface was blocked by bovine serum albumin (BSA), specific binding of the biotinylated Ag@Au nanoplates to streptavidin effectively enhanced the SPR signal to 1.56°, which is about 30-fold enhancement compared with direct immobilization. The amplification by the Ag@Au nanoplates demonstrated high specificity due to the biotin–streptavidin interaction, and the

hydroxy spacer molecule on the Ag@Au nanoplate surface contributed to the low nonspecific adsorption, as indicated by the control experiment (curve 2 in Figure 4c). For comparison, when Au nanoparticles ( $\approx 16$  nm) were used as enhancer, only limited amplification was observed (Figure 4d). The Au nanoparticles, which were functionalized with biotin tags by using the same procedure, enhanced the streptavidin binding signal to 0.15°, which is only three times better than direct streptavidin binding. Therefore, the amplifying effect of the Ag@Au nanoplates primarily stemmed from the Ag core rather than the outside Au coating. It is possible to adapt the Ag@Au nanostructures to many other systems, including sensors for DNA, RNA, peptides, and carbohydrates, by modifying them with different binding groups.

In summary, a high-performance SPR biosensing system has been enabled by using highly stable Ag@Au nanoplates as enhancers. The Ag nanoplates were stabilized by depositing a uniform thin layer of Au on the Ag surface while minimizing the disruptive galvanic-replacement reaction. The thin Au layer allows the plasmonic property of the original Ag nanoplates to be retained while preventing their contact with external etchants. The high stability of the protected nanoplates under various conditions allows multistep chemical modifications which are routinely needed for SPR sensing. Both the high stability and the

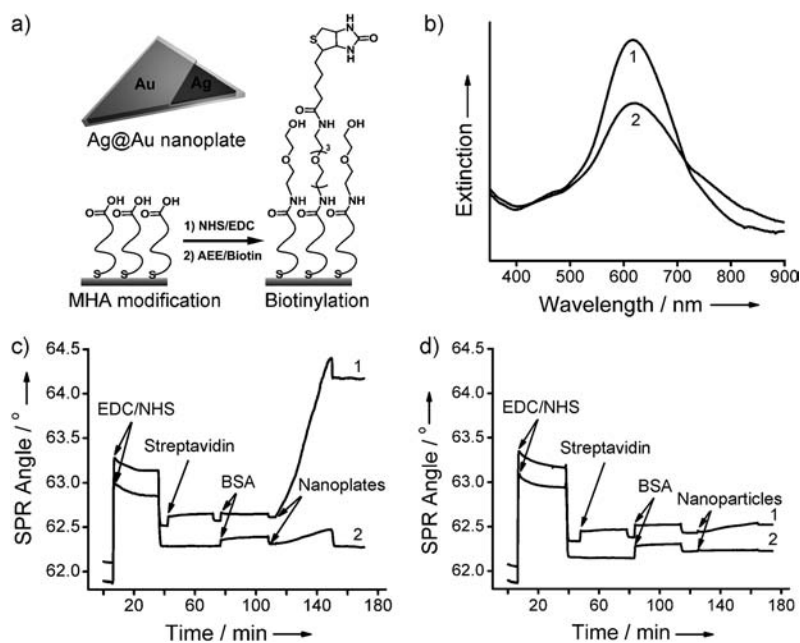


**Figure 4.** SPR sensing of streptavidin by using Ag@Au nanoplates. a) Modification of the Ag@Au nanoplates with biotin. b) UV/Vis spectra of the Ag@Au nanoplates 1) before and 2) after biotinylation. c) 1) Enhancement of SPR angle with the Ag@Au nanoplates as enhancers for detection of streptavidin, and 2) control experiment. d) 1) Enhancement of SPR angle with conventional Au nanoparticles (16 nm) as enhancers for detection of streptavidin, and 2) control experiment. c, d)  $c(\text{streptavidin}) = 0.5$  mg/mL,  $c(\text{BSA}) = 1$  mg/mL. Control experiments were carried out without addition of streptavidin in order to evaluate nonspecific binding of the particles on the substrate. AEE = 2-(2'-aminoethoxy)ethanol, EDC = 1-(3-dimethylaminopropyl)-3-ethylcarbodiimide hydrochloride, NHS = N-hydroxysuccinimide.

coupled with biotin through the carboxy groups of MHA, to prepare them for specific binding to streptavidin. Figure 4b shows the UV/Vis/NIR spectra of the Ag@Au nanoplates before and after biotinylation. The intensity of the plasmon band decreased to some extent, which can be attributed to the material loss typically associated with the repetitive centrifugation and washing processes during the multistep chemical modifications. The slight band broadening that can also be observed indicates slight aggregation of nanoplates after chemical modifications and redispersion in PBS solutions with a high salt concentration. The band position remained unchanged, thus confirming the chemical stability of the nanoplate structure. For comparison, when MHA-protected Ag nanoplates (without Au coating) were used, the nano-

plasmonic property account for the outstanding SPR sensing performance of the Ag@Au nanoplates. The highly stable Ag nanoplates are believed to hold great promise for fabricating a wide range of biosensors for detection of many other biomolecules, and may also find many interesting opportunities in the fields of biological labeling and imaging.

Received: December 20, 2011

Revised: March 15, 2012

Published online: April 24, 2012

**Keywords:** biosensors · gold · nanostructures · silver · surface plasmon resonance

- [1] a) R. Georgiadis, K. P. Peterlinz, A. W. Peterson, *J. Am. Chem. Soc.* **2000**, *122*, 3166–3173; b) M. A. Cooper, *Nat. Rev. Drug Discovery* **2002**, *1*, 515–528.
- [2] J. Wang, *Small* **2005**, *1*, 1036–1043.
- [3] a) M. Frascioni, C. Tortolini, F. Botrè, F. Mazzei, *Anal. Chem.* **2010**, *82*, 7335–7342; b) X. Shan, X. Huang, K. J. Foley, P. Zhang, K. Chen, S. Wang, N. Tao, *Anal. Chem.* **2010**, *81*, 234–240; c) A. Ambrosi, M. T. Castañeda, A. J. Killard, M. R. Smyth, S. Alegret, A. Merkoçi, *Anal. Chem.* **2007**, *79*, 5232–5240.
- [4] a) B. Wiley, Y. Sun, B. Mayers, Y. Xia, *Chem. Eur. J.* **2005**, *11*, 454–463; b) I. Pastoriza-Santos, L. M. Liz-Marzan, *J. Mater. Chem.* **2008**, *18*, 1724–1737; c) J. E. Millstone, S. J. Hurst, G. S. Metraux, J. I. Cutler, C. A. Mirkin, *Small* **2009**, *5*, 646–664.
- [5] a) Y. C. Cao, R. Jin, C. A. Mirkin, *Science* **2002**, *297*, 1536–1540; b) S. Nie, S. R. Emory, *Science* **1997**, *275*, 1102–1106.
- [6] K.-S. Lee, M. A. El-Sayed, *J. Phys. Chem. B* **2006**, *110*, 19220–19225.
- [7] a) D. Wodka, E. b. Bielańska, R. P. Socha, M. Elźbieciak-Wodka, J. Gurgul, P. Nowak, P. Warszyński, I. Kumakiri, *ACS Appl. Mater. Interfaces* **2010**, *2*, 1945–1953; b) P. Christopher, H. Xin, S. Linic, *Nat. Chem.* **2011**, *3*, 467–472.
- [8] J. Homola, S. S. Yee, G. Gauglitz, *Sens. Actuators B* **1999**, *54*, 3–15.
- [9] X. Jiang, Q. Zeng, A. Yu, *Langmuir* **2007**, *23*, 2218–2223.
- [10] Y. Chen, C. Wang, Z. Ma, Z. Su, *Nanotechnology* **2007**, *18*, 325602.
- [11] J. An, B. Tang, X. Zheng, J. Zhou, F. Dong, S. Xu, Y. Wang, B. Zhao, W. Xu, *J. Phys. Chem. C* **2008**, *112*, 15176–15182.
- [12] Q. Zhang, J. Ge, T. Pham, J. Goebel, Y. Hu, Z. Lu, Y. Yin, *Angew. Chem.* **2009**, *121*, 3568–3571; *Angew. Chem. Int. Ed.* **2009**, *48*, 3516–3519.
- [13] B. Tang, J. An, X. Zheng, S. Xu, D. Li, J. Zhou, B. Zhao, W. Xu, *J. Phys. Chem. C* **2008**, *112*, 18361–18367.
- [14] S. Gupta, S. Huda, P. K. Kilpatrick, O. D. Velev, *Anal. Chem.* **2007**, *79*, 3810–3820.
- [15] C. Xue, X. Chen, S. J. Hurst, C. A. Mirkin, *Adv. Mater.* **2007**, *19*, 4071–4074.
- [16] a) D. Aherne, D. E. Charles, M. E. Brennan-Fournet, J. M. Kelly, Y. K. Gun'ko, *Langmuir* **2009**, *25*, 10165–10173; b) M. M. Shahjamali, M. Bosman, S. Cao, X. Huang, S. Saadat, E. Martinsson, D. Aili, Y. Y. Tay, B. Liedberg, S. C. J. Loo, H. Zhang, F. Boey, C. Xue, *Adv. Funct. Mater.* **2012**, *22*, 849–854.
- [17] B.-H. Lee, M.-S. Hsu, Y.-C. Hsu, C.-W. Lo, C.-L. Huang, *J. Phys. Chem. C* **2010**, *114*, 6222–6227.
- [18] a) G. S. Métraux, Y. C. Cao, R. Jin, C. A. Mirkin, *Nano Lett.* **2003**, *3*, 519–522; b) Y. Sun, B. Mayers, Y. Xia, *Adv. Mater.* **2003**, *15*, 641–646; c) Y. Sun, Y. Xia, *J. Am. Chem. Soc.* **2004**, *126*, 3892–3901.
- [19] Y. Sun, Y. Wang, *Nano Lett.* **2011**, *11*, 4386–4392.
- [20] C. Gao, Q. Zhang, Z. Lu, Y. Yin, *J. Am. Chem. Soc.* **2011**, *133*, 19706–19709.
- [21] Q. Zhang, N. Li, J. Goebel, Z. D. Lu, Y. D. Yin, *J. Am. Chem. Soc.* **2011**, *133*, 18931–18939.
- [22] a) J. Zeng, X. Xia, M. Rycenga, P. Henneghan, Q. Li, Y. Xia, *Angew. Chem.* **2011**, *123*, 258–263; *Angew. Chem. Int. Ed.* **2011**, *50*, 244–249; b) Q. Zhang, Y. Hu, S. Guo, J. Goebel, Y. Yin, *Nano Lett.* **2010**, *10*, 5037–5042; c) Y. Sun, B. Gates, B. Mayers, Y. Xia, *Nano Lett.* **2002**, *2*, 165–168.